Assessment of Stormwater Discharge Contamination and Toxicity for a Cold-Climate Urban Landscape

Hayley Popick
University of Saskatchewan
Markus Brinkmann
University of Saskatchewan
Kerry McPhedran (kerry.mcphedran@usask.ca)
University of Saskatchewan https://orcid.org/0000-0001-9718-6793

Research Article

Keywords: Stormwater, polyaromatic hydrocarbons (PAHs), metals, cold climate, Raphidocelis subcapitata (algae), Vibrio fischeri (bacteria)

Posted Date: October 26th, 2021

DOI: https://doi.org/10.21203/rs.3.rs-944707/v1

Abstract

Background

Stormwater is water resulting from precipitation events and snowmelt running off the urban landscape, collecting in storm sewers, and typically being released into receiving water bodies through outfalls with minimal to no treatment. Despite a growing body of evidence observing its deleterious pollution impacts, stormwater management and treatment in cold climates remains limited, partly due to a lack of quality and loading data and modelling parameters. This study examines the quality of stormwater discharging during the summer season in a cold-climate, semi-arid Canadian city (Saskatoon, Saskatchewan).

Results

Seven stormwater outfalls with mixed-land-use urban catchments >100 km^2 were sampled for four summer (June-August 2019) storm events and analyzed for a suite of quality parameters, including total suspended solids (TSS), chemical oxygen demand (COD), dissolved organic carbon (DOC), metals, and targeted polyaromatic hydrocarbons (PAHs). In addition, assessment of stormwater toxicity was done using the two toxicity assays *Raphidocelis subcapitata* (algae) and *Vibrio fischeri* (bacteria). Notable single-event, single-outfall contaminant pulses included of arsenic (420 µg/L), cadmium (16.4 µg/L), zinc (924 µg/L), fluorene (4.95 µg/L), benzo[a]pyrene (0.949 µg/L), pyrene (0.934 µg/L), phenanthrene (1.39 µg/L), and anthracene (1.40 µg/L). The IC_{50} in both *R. subcapitata* and *V. fischeri* was observed, if at all, above expected toxicity thresholds for individual contaminant species.

Conclusions

In general, stormwater characteristics were similar to those of previous studies, with a bulk of contamination carried by the first volume of runoff, influenced by a combination of rainfall depth, antecedent dry period, land use, and activity within the catchment. Roads, highways, and industrial areas contribute the bulk of estimated contaminant loadings. More intensive sampling strategies are necessary to contextualize stormwater data in the context of contaminant and runoff volume peaks.

1.0 Introduction

Stormwater (SW) is water resulting from precipitation events and snowmelt, running off the urban landscape, collecting in storm sewers, and typically being released into receiving water bodies with little to no treatment. Continually increasing urbanization in cities worldwide seals soils, removes vegetation, and changes natural drainage paths. These changes lead to decreasing infiltration capacity of the local landscape and subsequent increases in the volume and flashiness (e.g., quickness of flooding) of SW runoff events (Barbosa et al. 2012; Blecken et al. 2012; Yang and Toor 2017). As SW flows over pavements, lawns, driveways, roads, and other urban surfaces, it accumulates high concentrations of

contaminants from both point and non-point sources. Thus, relative to natural waters, or even treated municipal sanitary wastewaters, the quality of SW effluents is generally poor (Barbosa et al. 2012; Blecken et al. 2012; Göbel et al. 2007; Gasperi et al. 2012; Zgheib et al. 2012).

A wide variety of contaminants are typically distributed across urban surfaces (i.e., non-point sources); however, they may also be present in single origins (i.e., point sources) that contribute to runoff quality. Contamination may include total suspended solids (TSS), total dissolved solids (TDS), nutrients (e.g., nitrogen, phosphorus), pathogens (bacteria, viruses, *Escherichia coli*), total and dissolved organic carbon (TOC/DOC), heavy metals, as well as organic chemicals like polyaromatic hydrocarbons (PAHs) (Aryal et al. 2010; Howitt et al. 2014; Zgheib et al. 2012; Winter et al. 2011; Yang and Toor 2017). These contaminants can also impact, and be impacted by, other water quality parameters, including pH, electrical conductivity (EC), turbidity (NTU), biological toxicity (indicated by IC_{10} or IC_{50} herein, see Methods for details), and chemical or biological oxygen demand (COD/BOD) (Björklund 2011; Howitt et al. 2014; Jartun et al. 2008; Järveläinen et al. 2017). For example, the solubility – and consequently aquatic toxicity – of heavy metals is dependent on parameters such as pH and TSS (Aryal et al. 2010; Göbel, Dierkes, and Coldewey 2007; Herngren et al. 2010; Milukaite et al. 2010; Rossi et al. 2013; Zgheib, Moilleron, and Chebbo 2012). The complexity of SW matrices makes defining their impacts equally complex since various contaminants may have additive, synergistic, or subtractive effects (Fulladosa et al. 2005). Overall, untreated SW is recognized as a significant transporter of municipal contaminants to receiving water bodies (Barbosa, Fernandes, and David 2012; Blecken et al. 2012; Matos, Bento, and Bentes 2015; Qinqin et al. 2015).

Untreated SW effluents can result in acute or chronic toxicity in receiving water bodies causing physiological effects in aquatic organisms, including impacts on growth, respiration, feeding habits, reproduction, and lethality at elevated concentrations (Mayer et al. 2011b; Rossi et al. 2013). For example, PAHs and metals – associated with organic matter and TSS, but fractions of which dissolve in SW – induce mortality at acutely toxic concentrations in *Raphidocelis subcapitata*, *Ceriodaphnia dubia*, and *Daphnia magna* (McGrath et al. 2005; Bragin et al. 2016). In addition, the bioaccumulation of contaminants can cause chronic toxicity at lower concentrations (Barbosa et al. 2012). Contaminants can accumulate in higher trophic levels, extending to humans, with metals/metalloids such as arsenic, copper, lead, and zinc associated with health effects including cancer, bone disease, hypertension, DNA and enzymatic dysfunction, nervous system damage, infertility, and organ failure (Chung, Yu, and Hong 2014; Ma et al. 2016; Zubala, Patro, and Boguta 2017). The potentially widespread distribution, coupled with severe impacts, of these SW contaminants necessitate establishing toxicity thresholds as parameters of SW quality which can be included in potential future SW regulations.

Land use (i.e., industrial, commercial, residential) impacts SW flow quantity and quality when considered in conjunction with climate, atmospheric, and catchment dependent variables. As mentioned previously, urbanized areas provide more contaminated and impervious surfaces leading to rapid discharge peaks and high runoff volumes (Barbosa et al. 2012; Sakson et al. 2018). For example, industrial land use has been observed to generate more TSS and metals related to roadways and galvanized buildings, while

residential and commercial areas generate more TOC and nutrients related to detergents and green space (Liu et al. 2013). Regardless of overall land use, roadways are significant sources of TSS and COD from pavement degradation (Huang et al. 2007). Vehicular activity further exaggerates road impacts with TSS-bound heavy metals, and PAHs linked to emissions, tire wear, and deterioration (Aryal et al. 2010; Björklund 2011; Legret and Pagotto 1999; Howitt et al. 2014). While metals are naturally-occurring geogenic elements present in sediments and soils predating industrialization (Owca et al. 2020), their mobilization in the urban environment is markedly increased by human activities (Soto et al. 2011; Sakson et al. 2018). Overall, SW is considered to be a more prevalent source of metals than other wastewaters (Barbosa et al. 2012).

Considering the complex influence of seasonal weather fluctuations and land use on SW quality, its management remains a concern for local governments. An effective management strategy relies on collecting local data to identify species and sources of contamination during runoff events. The assessment of the quality and quantity of the City of Saskatoon (CoS) stormwater runoff to the South Saskatchewan River (SSR) in Saskatoon, Saskatchewan, Canada, has been historically limited despite its potential to negatively impact the SSR and downstream municipalities (McLeod et al. 2006; Codling et al., 2020). Thus, the objectives of the current study are: (i) to obtain SW quality data for seven major catchments of the CoS by analyzing a suite of pollutants in field samples, including pH, EC, TDS, TSS, COD, DOC, metals, and targeted polyaromatic hydrocarbons (PAHs); (ii) compare the results to previous literature and regional SW quality data to assess SW quality patterns between or within storm events, or across land uses; (iii) determine the toxicity of the collected SWs on using two toxicity assays *Raphidocelis subcapitata* (algae) and *Vibrio fischeri* (bacteria); and (iv) considering the impact of land-use categories on catchment-level pollutant loading, to estimate the total pollutant loadings from urban runoff of these catchments into the SSR. The inclusion of toxicity assessment, in addition to the typical physicochemical and land-use SW parameters, is not common for SW assessment. Thus, this study will be valuable to determine toxicity which will be useful for informing future potential SW effluent guidelines.

2.0 Methods

2.1 Study Area

The City of Saskatoon (CoS) is located in central Saskatchewan and borders both banks of the South Saskatchewan River (SSR). With a total area of 228.1 km^2 and a population of about 330,000, it is the largest municipality in Saskatchewan, located in western Canada (Statistics Canada 2021). Based on climate data collected by the Saskatchewan Research Council's Climate Reference Station (CRS), the average daily temperature ranges between approximately 18.7°C in August and -14.7°C in January, with an annual average of 3°C. The CoS receives an average of 355 mm of precipitation per year, with ~50 mm of precipitation falling between the months of November and March as snowfall. The CoS collects rainfall data from eight rain gauges (Al Masum et al., 2021) with relevant rain gauges used currently to

estimate the individual catchment stormwater volumes and pollutant concentrations. As in many municipalities, the CoS rainfall is often localized making the use of relevant gauges important in the determination of reasonably accurate rainfall volumes.

Of the CoS storm sewers, seven outfalls with large catchment areas (>1 km^2) are considered in the current study. These seven catchment areas are delineated in the Supporting Information (SI) Figure S1 while sampling outfall locations are presented in Figure 1. The sampling outfalls chosen for this study (CoS naming conventions in brackets) include those at Circle Bridge on the east side (S. Circle Dr. Bridge East (**SCB E**)) and west (S. Circle Dr. Bridge West (**SCB W**)) banks; outfalls close to the CoS central business district (**MacPherson Ave**.; **14th St. E**.; **17th St. W**.; **23rd St. E**.), and one outfall located in the north end of the city (**Silverwood Dog Park**). These outfalls are identified with blue markers, while red markers denote snow storage facilities which were sampled as part of a parallel study (Figure 1).

Table 1
Overview of analyzed stormwater quality parameters for the 2019 sampling season. Parameters are grouped by sampling event (date) with average (standard deviation) across seven sites presented for each sampling event. Table S2 includes individual outfall information for each of these sampling events.

Date	Sites	pH	TDS	EC	DOC	COD	TSS
		(-)	(mg/L)	(µS/cm)	(mg/L)	(mg/L)	(mg/L)
June 12, 2019	7	8.12 (0.90)	648 (378)	1,296 (733)	36.2 (22.6)	289 (229)	129 (105)
June 20, 2019	7	9.18 (0.52)	375 (114)	768 (228)	12.8 (4.4)	246 (168)	451 (315)
July 25, 2019	7	8.19 (0.10)	326 (145)	667 (290)	12.8 (4.1)	93.1 (27.4)	44.1 (22.8)
August 22, 2019	7	6.48 (1.00)	346 (235)	707 (468)	154 (145)	1,401 (743)	494 (386)
Average (SD)	**7**	**7.99 (1.12)**	**424 (151)**	**859 (294)**	**53.9 (67.5)**	**508 (602)**	**280 (226)**

2.2 Sampling and Laboratory Analyses

Grab sampling was used to collect SW from seven outfalls during four wet weather events between June and August 2019. This method of SW sampling has traditionally been the most common due to its simplicity and accessibility (Zhang et al. 2008; Zawilski et al. 2014); however, drawbacks of this method include the ability only to determine instantaneous pollutant concentrations and the potential for variations in composition occurring prior to laboratory analysis, i.e., during sample transport (Zhang et al. 2008). Sampling only occurred during storm events if <3 mm of rainfall was observed 48 hours prior to the onset of the storm to allow contaminants to accumulate on land surfaces. Sampling commenced

within the first 30 minutes of the storm (except July 25, where sampling occurred the morning after the storm due to safety concerns of night sampling). Outfalls were approached from above, and a sampling pail was lowered into the SW flow close to the mouth of the outfall. Collected samples were then transferred into 4-L and 1-L Nalgene containers. Samples were sealed, labelled, and transported back to the University of Saskatchewan (USask) Environmental Engineering labs, where they were stored at 4°C prior to analysis.

Several physicochemical, biological, and toxicity parameters were selected to assess the SW quality. The physicochemical analyses included pH, TSS, TDS, EC, COD, TOC/DOC, metals, and PAHs. The biological analyses comprised the enumeration of fecal coliforms, while two standardized laboratory toxicity assays were conducted with *Raphidocelis subcapitata* algae and *Vibrio fischeri* bacteria.

2.2.1 Physicochemical Analyses

The TSS concentration was measured *via* vacuum filtration by following Standard Methods 2540 (“2540 SOLIDS” 2018), using Whatman™ 934-AH™ glass microfibre filters (1.5 µm). A HACH sensION 156 digital probe was used to measure the pH, TDS, and EC of the samples. To analyze DOC, all samples were extracted through a 0.45-µm Teflon filter using a Luer-Lock 12-mL syringe. Approximately 40 mL of filtered sample was placed in a glass vial and measured with a Lotix combustion TOC analyzer (Teledyne Tekmer, OH, USA) following the manufacturer-provided method. To measure COD, samples were added to VWR Mercury-Free High-Range (20-1,500 mg/L) COD digestion vials following the HACH COD Method 8000 (HACH 2014). Samples were run in duplicate using either 2 mL of sample or 1 mL of sample and 1 mL of distilled (DI) water. Afterward, the COD was measured using a HACH DR/4000U Spectrophotometer (HACH USA, CO, USA) set to 625 nm.

For metals analysis, samples were acidified using 0.02 N nitric acid and vacuum-filtered through a 0.45-µm nitrocellulose filter. A 100-mL sample volume was passed through the filter and the filtrate collected in a Nalgene container. Samples were analyzed using Inductively Coupled Plasma Mass Spectrometry (ICP-MS) at the USask Department of Geological Sciences or the USask Toxicology Centre. The methods at the Department of Geological Sciences included the use of the PerkinElmer 300D ICP-MS, diluting samples 20x prior to analysis and using a custom calibration standard (SCP Science) for blanks and standards of 10, 50, and 100 ppb. The certified reference material was NIST-SRM1643f. At the Toxicology Centre, samples were analyzed using an Agilent 8800 ICP-MS QQQ Triple Quadrupole mass spectrometer (Agilent, Santa Clara, USA). OmniTrace Ultra nitric acid (HNO_3) (w/w) (Millipore-Sigma, Ontario, Canada) was used for blanks, standards, and sample solutions. High-purity standard stock solutions (1,000 mg/L) were purchased from Delta Scientific (Mississauga, Canada). The calibration standard solution containing 22 multi-elements was supplied by SCP Science (Quebec, Canada). The standard reference material, natural water 1640a, was supplied by the National Institute of Standards and Technology (NIST) (Gaithersburg, USA). Limits of detection and quantification for each method are included in Table SI-B3.

Samples for PAH analyses were pre-filtered (WhatmanTM GF/F glass microfibre filters (0.7 µm) to remove high TSS concentrations prior to solid-phase extraction (SPE) to eliminate clogging of the filter. After filtration, 2 mL of chloroform was added per 1 L of sample as a preservative, with the samples stored in amber glass bottles at 4°C prior to extraction. A deuterium-labelled internal standard mix (500 mg/L of acenaphthene-d_{10}, chrysene-d_{12}, and phenanthrene-d_{10} in acetone) provided by Sigma Aldrich (Oakville, ON) was added to the sample at a 10 µL/L ratio. Before sample addition, Waters Oasis HLB 500 mg extraction columns were pre-conditioned using 3 mL dichloromethane (DCM), 3 mL methanol (LC-MS grade), and 3 mL 18.2 MΩ-cm ultrapure water (EMD Milli-Pore Synergy® system, Etobicoke, ON). Up to 500 mL of each SW sample were vacuum-extracted through the column at a rate of 1 drop/second. After extraction, the column was washed with 3 mL of 5% methanol in water and air-dried with suction for 10-30 minutes. If column elution was not possible immediately following extraction, the columns were stored at -20°C. Columns were eluted twice with 5 mL of DCM and once with 5 mL of methanol. The eluate was collected in glass vials, reduced to a volume of 10 mL with a gentle stream of nitrogen gas, and split into two 5-mL portions (one portion used for a parallel research study). The aliquots were reduced to near dryness under nitrogen and reconstituted in 0.5 mL nonane. The reconstituted samples were added to gas chromatography vials and stored at 4°C until analyzed. Samples were analyzed for PAH concentrations using Gas Chromatography-Mass Spectrometry (GC-MS). A Thermo Trace 1300 gas chromatograph with a Thermo ISQ 7000 quadrupole mass detector was used for analysis. Helium (99.999% purity) was used as the carrier gas to separate the PAHs using an Agilent DB-5ms (60 m x 250 µm I.D., film thickness 0.1 µm) fused silica capillary column. Limits of detection and quantification for each method are included in Table S1.

2.2.2 Biological Analysis

Coliforms were enumerated using two different media: m-ColiBlue24 Broth PourRite Ampules (HACH USA, CO, USA) added to Fischer-Scientific Petri dishes and 3M Petrifilm *E. coli* film plates. Samples added to Petri dishes were first processed *via* a membrane filtration method (HACH 2019). Petrifilm samples were prepared by adding 1 mL of unfiltered sample directly to the Petrifilm according to manufacturer-provided methods (3M Food Safety 2017). All samples were incubated at 37.5°C for 24 hours before colony-forming units (CFUs) were enumerated.

2.2.3 Toxicity Analyses

The first toxicity assay included inhibition of the luminescence of *V. fischeri* aquatic bacteria. The method used is described in EPS RM/1/24 (Environment Canada 1993) using a Microtox M500 instrument (Modern Water, DE, USA). The Osmotic Adjustment Solution (OAS) required to ensure freshwater samples possess appropriate salinity for the marine bacteria was used as recommended in the methods. Phenol (60 mg/L) was used as a positive control and 20% sucrose as the diluent (SD) as recommended in the RM/1/24 protocol for freshwater samples for increased test sensitivity to metals. The SD was also used as the negative control. This method was adapted to measure the luminescence inhibition of dilution series in 96-well microplates using an OptimaSTAR plate analyzer. Prior to the test, 10 mL each of the samples, OAS and SD were refrigerated for one hour before being transferred to 25-mL beakers. Plates

were run both inoculated and uninoculated to correct for background luminescence. To inoculate the wells, 1 mL of Microtox Reconstitution Solution was mixed with a vial of lyophilized *V. fischeri* strain NRRL B-11177 (Modern Water, USA); 0.3 mL of this solution was further diluted with 3 mL of SD. This solution was placed in a multichannel pipette reservoir on ice. Placing the plates on a paper towel over ice and using a multi-pipettor, plates were inoculated with 8 µL of the bacteria solution. Luminescence readings were taken immediately, after 5 minutes, and after 15 minutes, with plates remaining on ice between measurements. Due to the configuration of the plates, samples and standard were run in triplicate as seven-step dilutions while the phenol was a six-step dilution series. Values for both samples and phenol are reported as the IC_{50} and IC_{10} relative to the negative control at 15 minutes.

The second bioassay included 72-hr chronic toxicity of SW to *R. subcapitata* green algae following the protocol outlined in the EPA Method 1003.0 (EPA 2002). Prior to analysis, a dilution series of inoculated algae stock was used to establish a linear relationship between fluorescence and cell count. Samples were prepared in 1-mL wells of 24-well microplates in a configuration of four replicates of a stock negative control and a five-step dilution series. Wells were inoculated with 100 µL of inoculum (1,000,000 cells/mL) as prepared according to the protocol to meet appropriate cell densities (10,000 cells/mL in wells at the start of the test). Using fluorescence as a proxy for algae cell count, growth inhibition was measured as a function of fluorescence at 0 h and at 72 h. Cell counts were verified directly from one random control well per plate at 0 h to ensure proper inoculation. Both algae fluorescence and cell counts were read using the Tecan Spark® multifunction plate reader (Tecan Trading AG, Switzerland). Sample concentration in wells ranged from 100–6.25%, both inoculated and uninoculated to account for background fluorescence. Initially, the IC_{50} at 72 hours was calculated; as the IC_{50} was not observed at full concentration for all samples, the IC_{10} was additionally calculated (see Statistical Analysis).

2.3 Rainfall, Runoff Coefficients, and Site Mean Concentration (SMC) Values

Breakdowns of individual land-use areas within each of the seven CoS catchments have been previously determined (Al Masum et al., 2021) and are included currently in Figure S2. Please consult Al Masum et al. (2021) for further information on this delineation and calculations which will only be covered briefly herein. To determine SW outfall loadings (*L*) into the SSR values needed to be determined including the individual catchment runoff coefficients (*CR*), the precipitation (*P*), and the site mean concentration (*SMC*).

The land-use classifications considered herein are presented in Table S2 including eight classes of single-family residential (SR), multi-family residential (MR), roads (R), highways (HW), commercial (CM), industrial (IN), green (GR), and agricultural (AG). Each of these classifications has been designated a runoff coefficient value by the CoS. The individual catchment land-use area overall runoff coefficient values were calculated using Figure S2 and Table S2 information for use in the loading calculations. The precipitation data for the CoS was taken from rain gauge data available as discussed in Section 2.1.

Each rainfall event's individual pollutant concentration is used to calculate an event mean concentration (EMC) by dividing the total pollutant mass by the total event volume. Using this information, a site mean concentration (SMC) is the geometric mean of multiple rainfall events' EMC over a time interval (Charbeneau & Barrett, 1998; US EPA, 1983). This interval was 6 months, April through September, for the current study, given this is the typical rainfall season for the COS. The SMC is considered the most accurate measure of the average pollutant concentrations as it is measured as event-volume-weighted mean values of EMCs (Järveläinen et al., 2017). There is no existing SMC data for the current study catchment areas so SMC values were considered based on averages of land use classifications found in previous studies, including Melanen (1981), Mitchell (2005), Nordeidet et al. (2004), and Jarvelainen et al. (2017) (Table S3).

Following the modeling methods of Järveläinen et al. (2017), equations (1) and (2) were used to calculate monthly pollutant loads:

$$L_{ua} = CR \cdot P \cdot SMC \quad (1)$$

Where L_{ua} (kg/km^2) is the monthly unit area load, CR (dimensionless) is the runoff coefficient (outlined in Table 1), P (mm) is the monthly precipitation depth, and SMC (mg/L) is the characteristic event-volume weight SMC.

$$L_{tot} = L_{ua} \cdot A \quad (2)$$

Where L_{tot} (kg) is the monthly pollutant export rate, and A (km^2) is the total area occupied by the individual land use class.

2.4 Statistical Analysis

To prepare the algae and Microtox data for statistical analysis, the background fluorescence or luminescence of uninoculated samples was subtracted from that of inoculated samples to remove any baseline fluorescence/luminescence. The exponential growth rate between the initial and endpoints was calculated and normalized as a percent of the average growth observed in the negative control for both procedures. With a normalized growth and luminescence inhibition determined for every dilution series, the datasets could be transferred to GraphPad Prism 9 (GraphPad Software, San Diego, CA) for statistical analysis. Within GraphPad Prism, four-parameter logistic regression was used to fit curves to the growth rate inhibition data to obtain the 72-hour (for algae) or 5- and 15-minute (for Microtox) IC_{50} values and related 95% confidence intervals (CI) for each analyzed sample. As the IC_{50} was not observed for many algae samples, the IC_{10} and its 95% CI was also interpolated from the curve. These results were then used for one-way analysis of variance (ANOVA) with Tukey's ad-hoc tests, correlation, and t-test analyses.

3.0 Results And Discussion

The Results and Discussion will be considered in three sections including: (1) Physicochemical data; (2) Toxicity data; and (3) Land-use management. The physicochemical analyses section will include a discussion of results in four subsections, with one covering the pH, TDS, and EC; a second for DOC, COD, and TSS; a third for *E. coli*, and the fourth including metals and PAHs. The toxicity section presents the two toxicity assays *R. subcapitata* and *V. fischeri*. The final land-use section will be used to discuss the impacts of land-use on the individual catchment area estimated pollutant loadings into the SSR. Figure 1 presents a map of the CoS and a summary of all physicochemical, metals, and PAH data in the form of box and whisker plots. Further details will be discussed in each of the following subsections.

3.1 Physicochemical data

A summary of all physicochemical data grouped by the four sampling dates (with seven sites each) is presented in Table 1 with a summary of all data collected shown in box-and-whisker plots in Figure 1. In addition, a summary of data grouped by sampling site (Table S4) and outfall-specific data grouped by sampling date (Table S5) are presented in the Supporting Information (SI).

3.1.1 pH, Total Dissolved Solids (TDS), and Electrical Conductivity (EC)

The overall average summarized pH, TDS, and EC values for all samples collected in 2019 were 7.99, 424 mg/L, and 859 µS/cm, respectively (Table 1). Event-average pH values were highest on the June 20 sampling date with an average of pH 9.18 (Table S5). Significantly lower pH values relative to all events occurred on August 22 (average pH 6.48) ($p \leq 0.05$). No significant difference was found relative to the July 25 or June 12 samples, likely due to the pH range observed on these dates (pH 7.02-9.52). Large pH ranges were also observed on August 22 despite the lower overall pH values, with a low pH of 5.09 for 17th St. W and a high pH of 7.94 for SCB W (Table S5). These values were both markedly lower than the average values for each of these sites of pH 7.39 and 8.44, respectively. Lower pH values for August 22 samples are likely related to road tar application performed by the CoS in the days immediately before the storm event. Overall, the pH variability appears to be more closely associated with the sampling date than the specific outfall being sampled; however, there are still differences between the individual outfalls, which will be more closely considered in the Land-use management Section 3.3.

The TDS and EC are typically associated parameters; therefore, they will be discussed together in this section. The range of TDS over the entire year is comparable to that observed in other cold climates (Taka et al. 2017). The June 12 sampling date produced the highest average values for both parameters with 648 mg/L and 1,296 µS/cm, respectively, but there was no significant difference in the dataset relative to other events ($p \leq 0.05$). However, the elevated concentrations on June 12 were largely due to two sites in particular, including SCB E (974 mg/L and 1,914 µS/cm) and 23rd St. E. (1,295 mg/L and 2,550 µS/cm), respectively (Table S5). Unlike the pH, the EC and TDS concentrations were elevated at these two sites in general for all sampling dates (Table S4). Low-volume flow has been observed consistently at these outfalls during dry-weather sampling and surveying, and pipe corrosion may contribute to these

differences. Nearby traffic surfaces also potentially contribute TDS at minimal runoff volumes (see Land-use management section). If these sites are removed, the June 12 EC and TDS (922 µS/cm and 454 mg/L) remain elevated compared to the other three events. The average EC and TDS values of July 25 samples are within 14% of the average values of June 20 and August 22 samples, despite the variation observed across other parameters. Sampling June 20 and August 22 near the flow peak (with higher volumes diluting TSS) or near the contamination peak (with high TSS concentrations efficiently binding TDS) may explain the relative similarity in their TDS values to July 25.

The two storm events with the greatest TSS, June 20 and August 22, also possessed the highest and lowest average pH values, respectively (Table S5). The high concentration of TSS relative to other contaminant species (notably EC and TDS, which are comparable in June 20 and August 22 samples to the low-TSS July 25 event) and its event-specific origins may explain the difference. High pH in spring or early summer events is likely contributed by spring weathering of traffic surfaces, as high pH and alkalinity have been observed alongside high TSS in roadside snowbanks (Moghadas et al. 2015). Furthermore, concrete surfaces – regardless of use – contribute eroded particles to alkaline SWs. Previous studies found SW pH increased from 7.0-7.3 to 8.1-9.3 in all test SWs when conveyed in a concrete sewage pipe (Borris et al. 2017) and from 7.4 to 7.8-8.6 after infiltrating a porous cement pavement (Kuang and Sansalone 2011). Thus, the high-intensity June 20 storm likely contained eroded concrete particles at the time of sampling. This could explain why average June 20 pH was elevated across all samples relative to other events (Table 1), as high-rainfall-intensity TSS erosion would have been captured during the sampling event (while the June 12 event was low-intensity and the peak of the July 24 event was missed).

Relatedly, it is assumed uptake of road tar and its associated metals and chlorinated organic compounds contributed to SW acidification during the August 22 event: low pH values in August samples are accompanied by twofold greater concentrations of dissolved aluminum and iron relative to all other sampled events (see Figure 2 and Section 3.1.4), which have been previously associated with higher concentrations of chloride and lower pH values in SWs (Bäckström et al. 2004; Reinosdotter and Viklander 2005). Though chloride testing of the current SW samples was limited, the August 22 SCB E sample contained more chloride than all June 12 and July 25 samples tested (Table S6). In cold climates, TDS and EC are a major toxicity concern due to the practice of road salting in the winter months. Mayer et al. (2011a) found elevated EC and chloride concentrations of 2,000-21,500 µS/cm and up to 19,135 mg/L, respectively, in early spring runoff; by late spring through fall, the chloride concentration had decreased to 4-185 mg/L. Masoner et al. (2019) reported a relatively low chloride ion concentration of 0.82-196 mg/L in temperate-climate SW, which is comparable to the summer value reported by Mayer et al. (2011a). With the exception of the August 22 samples, the SW in this study falls into the same range as these previous observations. Neither study reports TDS, though Masoner et al. (2019) report a 38-1,074 µS/cm range similar to the summer SW in this study. Mayer et al. (2011a) report winter and early spring EC values of 2,000-21,500 µS/cm. As no early spring storm events occurred over the study period due to an extensive period without rainfall, this implies a brief seasonal window in which SW runoff (as opposed to snowmelt) may exhibit elevated TDS and EC.

3.1.2 Dissolved Organic Carbon (DOC), Chemical Oxygen Demand (COD), and Total Suspended Solids (TSS)

The average overall summarized DOC, COD, and TSS were 53.9 mg/L, 508 mg/L, and 280 mg/L, respectively (Table 1). Each of these parameters had maximum average values on August 22 with 154 mg/L, 1,401 mg/L, and 494 mg/L, respectively, and minimum average values on July 25 with 12.8 mg/L, 93.1 mg/L, and 44.1 mg/L, respectively (Table S5). The DOC and COD were significantly higher on August 22 relative to other events, while the TSS were significantly higher on June 20 and August 22 relative to July 25, but not June 12 ($p \leq 0.05$) (Table S5). Despite the high concentrations on August 22 overall, the individual sites had wide ranges in concentrations, including 12.1-378 mg/L for DOC, 388-1,847 mg/L for COD, and 97-1,304 mg/L for TSS (Table S4). Relative to the August event, the ranges for DOC, COD, and TSS on the other three sampling days were 3.14-13.3%, 5.04-45.3%, and 5.76-79.7% smaller, respectively. In addition, the site-specific data indicate a clear trend with the MacPherson Ave., 14th St. E., 17th St. W., and 23rd St. E. having elevated concentrations for these parameters versus the lower concentrations for SCB E, SCB W, and Silverwood Dog Park (Table S5). Clearly, these parameters vary in both temporal (sampling date) and spatial (site) metrics.

While BOD and COD are commonly used to measure wastewater quality, measuring the actual organic carbon content is increasingly preferred as techniques for extracting and measuring TOC and DOC become more accessible. As DOC values for the June 20 and July 25 events are comparable, the contaminant peak of these and the June 12 event may have been missed (Table 1). Samples from outfalls located near the geographic centre of the CoS displayed a fivefold increase in DOC concentration on June 12 as compared to June 20; these same outfalls possessed the upper range of DOC concentrations observed on August 22 (Table S5). Relatively larger proportions of residential and commercial land use in city-centre catchments likely contribute to elevated DOC and COD. The June and July samples possess COD ranges comparable to other SWs: Lee et al. (2011) found a COD range of 10-360 mg/L per storm event, and Zhang et al. (2013) observed COD event concentration peaks between 400-750 mg/L. Lee and Bang (2000) found COD ranges of 13-2,796 mg/L for residential areas and 10-810 mg/L for industrial areas, similar to August samples in this study. As previously discussed with respect to pH, road tarring occurred the day before the August 22 event with significant quality impact: organic contaminants related to tar particles are reflected by overall higher concentrations for DOC, COD, and TSS and more acidic pH for this sampling event (Zhang et al. 2013).

The relatively low TSS of the July 25 event might be due to sampling after the bulk of the runoff had already entered the SSR. Across the CoS, the June 12 event had low rainfall depth relative to the June 20 event. The lack of intensity or runoff volume likely explains the difference in average TSS between the two events. Milukaite et al. (2010) found an average TSS of 920 mg/L with a range of 48-3,640 mg/L, comparable to ranges of 8.3-2,796 mg/L found in separated sewers by Lee and Bang (2000) and 34-2,288 mg/L found in cold-climate highway runoff by Mayer et al. (2011a). COD values of 14-320 mg/L (Zgheib et al. (2012) and 70-1,455 mg/L (Lee and Bang 2000), which are ranges comparable to those

observed in this study. Somewhat lower TSS (66-937 mg/L) and COD (63-146 mg/L) ranges were compiled across multiple sources of literature by Göbel et al. (2007); however, these datasets were published between 1975-2001, and SW quality has since changed significantly (Westerlund and Viklander 2008).

3.1.3 Coliform analysis

The highest average coliform values were for the August 22 sampling at 4,625 CFU/100 mL, followed closely by the July 25 value of 4,688 CFU/100 mL (Table S5). The remaining two sampling dates were lower at 794 and 272 CFU/100 mL for June 20 and June 12, respectively, though no significant difference was observed ($p \leq 0.05$). On a site basis, there were four sites with averages exceeding 2,000 CFU/100 mL, including SCB W (2,283 CFU/100 mL), MacPherson Ave. (5,963 CFU/100 mL), 14th St. E. (4,070 CFU/100 mL), and 23rd St. E. (5,000 CFU/100 mL) (Table S4). In contrast, the remaining three sites, including SCB E, 17th St. W, and Silverwood Dog Park, had averages below 400 CFU/100 mL. Coliform concentrations varied widely when present, for example, the MacPherson Ave. and 23rd St. E sampling sites had ranges of <1 to >9,999 CFU/100 mL over the four sampling dates. Overall, no clear trends could be determined based on the current results.

The ranges of enumerable coliforms observed in this study are comparable to a previously-reported range of 388 to >16,000 *E. coli*/100 mL (Harmel et al. 2016). Selvakumar and Borst (2006) reported a range of 1,500-8,500 *E. coli*/100 mL, where land use did not significantly influence *E. coli* concentrations, but coliform concentration increased with impervious surface density, an observation they corroborated with previous literature. Health Canada's Guidelines for Canadian Recreational Water Quality (2012) are ≤ 200 *E. coli*/100 mL for the geometric mean concentration of five samples and ≤ 400 *E. coli*/100 mL for a single sample maximum concentration. The Saskatchewan Water Security Agency recommends in their Sewage Works Design Standard (2012) an objective of ≤ 200 *E.* coli/100 mL fecal coliform concentrations in treated wastewater effluent. Such high variability between events was similarly observed by McCarthy et al. (2011), who found neither antecedent dry period nor storm intensity explained this variability. Dry-weather outfall sampling in summer 2018 has previously reflected relatively high coliforms at the 23rd St. E outfall, but not at the 14th St. E outfall; there may be persistent or emerging coliform sources along the reach to the outlet. Generally, coliform/*E. coli* results appear to not be informative and may be of minor value for determination in future SW studies.

3.1.4 Heavy metals and polyaromatic hydrocarbons (PAHs)

A total of 18 metals were identified at detectable concentrations in SW samples as summarized in Figure 2 with all sampling data for individual dates and outfalls shown in Table S7. Generally, aluminum, copper, iron, manganese, strontium, and zinc were present in all samples. Dissolved arsenic, copper, and zinc results regularly exceeded Canadian Council of Ministers of the Environment (CCME) guidelines (2009) as shown in Table S7, with threshold-exceeding spikes observed for aluminum, cadmium, iron, and lead. Copper was generally an order of magnitude higher in June 12 samples relative to later-season samples; conversely, zinc concentrations were elevated in July and August relative to June. Aluminum and iron

concentrations follow an overall trend of August 22 > June 20 > June 12 > July 25. Notable contamination events include discharges of strontium from the SCB E outfall on June 12 (782 µg/L) and the SCB W outfall on August 22 (3,463 µg/L); a discharge of arsenic from the 23rd St. E. outfall on June 12 (420 µg/L); and two discharges of zinc from the Silverwood Dog Park catchment on July 25 and August 22 (541 µg/L and 924 µg/L respectively).

The trends in aluminum and iron may reflect first flush behaviour for these parameters, though August 22 concentrations may be elevated due to road tar application. Arsenic and strontium spikes in June 12 samples may derive from spring-weathered preserved wood (arsenic) or flares, greases, and fresh concrete (strontium). The two spikes of zinc from the Silverwood Dog Park catchment imply potential point-source releases from industrial land use. Seasonal trends in copper and zinc concentrations have been previously observed (Mangani et al. 2005); additionally, zinc and copper have commonly been found to have the highest concentration of all metals in SW (Gasperi et al. 2012; Zgheib et al. 2012; Sakson et al. 2018; Davis et al. 2001; Gunawardena et al. 2013). Elevated zinc levels have been connected with galvanized SW sewer pipes (Borris et al. 2017). This was generally consistent with the data, though aluminum and iron were often more abundant, potentially as a reflection of local geogenic concentrations (Owca et al. 2020). Mayer et al. (2011a), Galfi et al. (2017), Sakson et al. (2018), and Zgheib et al. (2012) report similar ranges across cadmium, chromium, copper, iron, and zinc, but the latter two found lead concentrations an order of magnitude greater, compared to this study.

A total of 13 PAHs were identified at detectable concentrations as summarized in Figure 3 with all sampling data for individual dates and outfalls shown in Table S8. The $\sum$PAHs was generally below 1 µg/L in the dissolved fraction of SW samples. Fluorene was abundant in the SCB E June 12 sample, the 14th St. E. July 25 sample, and most notably, the 23rd St. E. July 25. Concentrations of anthracene, pyrene, and benzo[*a*]pyrene exceeded the CCME guidelines (Table S8). Fewer samples exceeded the threshold for benz[*a*]anthracene, and only the SCB W June 12 and 23rd St. E. July 25 samples contained threshold-exceeding amounts of fluorene and phenanthrene.

PAHs in this study were comparable to combined dissolved and particulate findings by Zgheib et al. (2012). Mayer et al. (2011a) observed that aqueous PAHs were below instrument detection limits and that 91% of PAHs were particulate-bound. Particle-bound PAHs tend to have high molecular weight (Aryal et al. 2010; Gasperi et al. 2012; Masoner et al. 2019; Rentz et al. 2011; Zgheib et al. 2012), while low-molecular-weight PAHs predominantly are found in dissolved phases (Gasperi et al. 2012). This would explain some of the unremarkable PAH concentrations found in filtered SW samples, especially high-TSS August 22 samples, as the bulk of PAHs would remain within the filter sediment. The hydrophilic nature of LMW PAHs may also explain the elevated PAHs in July 25 samples relative to August 22: the high presence of benzo[*ghi*]perylene, fluorene, and phenanthrene present in the July 25 samples likely originated from roadway degradation; however, this was not observed in the August 22 samples. This is likely due to sampling timing; the storm preceding sampling on July 25 likely had mobilized dissolved PAHs by prolonged water exposure.

3.2 Toxicity assessment

3.2.1 Algae Bioassay

All samples were filtered (see Methods) prior to testing, therefore all particle-bound contaminants were removed prior to testing. The 72-hour growth rate of *R. subcapitata* satisfied the test validity requirements of the EPA method. Of the 16 samples tested for algal growth inhibition, 5 produced a toxic response (Table 2). Most samples did not inhibit algal growth by more than 20% at full concentration and all concentrations in the diluted series stimulated similar growth to negative controls. Most toxic samples were from the June 12 event, with one each from the July 25 and August 22 events. All samples originated from different outfalls; however, samples from the 17th St. W outfall exhibited an IC_{50} below 33% concentration on both June 12 and August 22. Interestingly, the August 22 Silverwood Dog Park sample did not induce a toxic response, though it contained nearly twice the concentration of zinc from the outfall's response-inducing July 25 sample. Pearson's correlations between the IC_{10} and DOC, chloride, and individual metals and PAHs, respectively, only found correlations for cadmium ($r = 0.693$).

Table 2

The 72-hour growth inhibition EC_{50} and EC_{10} for algae (*R. subcapitata*) and 5- and 15-minute IC_{50} for Microtox (*V. fischeri*). Results are presented as percent of total sample concentration required to read the endpoint. EC_{50} and EC_{10} values were generated using GraphPad Prism as a dose-response curve (see Methods) of, in the case of *R. subcapitata*, the initial (t = 0) fluorescence observed after 72 hours, and in the case of *V. fischeri*, normalized luminescence as a percent of the negative control.

Sampling Date	Sampling Site Name	Algae		Microtox	
		EC_{50} (CI 95%)	**EC_{10} (CI 95%)**	**$IC_{50-5\ min}$ (CI 95%)**	**$IC_{50-15\ min}$ (CI 95%)**
June 12	SCB E	92.1 (79.9-114)	30.5 (22.0-41.2)	-	-
	MacPherson Ave	ND	100 (NC)	49.6 (15.6->100)	60.8 (18.9->100)
	17th St W	81.9 (73.8-92.1)	31.6 (24.9-40.0)	ND	52.6 (NC)
	23rd St E	101 (92.5-114)	47.9 (37.9-59.3)	NC	52.3 (NC)
June 20	23rd St E	ND	97.7 (33.8-100)	ND	57.6 (NC)
	Silverwood Dog Park	-	-	ND	58.6 (45.0-71.2)
July 25	SCB E	-	-	28.5 (16.3-54.9)	44.8 (28.2-72.3)
	MacPherson Ave	ND	76.4 (56.1-88.6)	ND	ND
	14th St E	-	-	79.2 (59.5-98.7)	52.0 (NC)
	23rd St E	ND	90.7 (26.0-100)	ND	71.3 (NC)
	Silverwood Dog Park	109(98.3-127)	35.3 (23.6-44.0)	ND	52.7 (NC)
August 22	SCB W	ND	85.9 (60.8-96.2)	ND	ND (33.92-NC)
	MacPherson Ave	95.0 (68.7-180)	16.6 (8.1-30.5)	62.0 (28.5-ND)	60.7 (42.5-NC)
	14th St E	ND	ND	49.6 (15.6-ND)	60.8 (18.9-ND)

ND – no observable toxicity detected at the respective threshold.; NC – not calculated; - – sample not tested.

17th St W	ND	24.4 (13.1-37.3)	88.2 (69.0-143)	53.9 (NC-59.6)
23rd St E	ND	ND	ND	29.6 (19.9-45.3)
Silverwood Dog Park	ND	ND	ND	52.8 (NC)

ND – no observable toxicity detected at the respective threshold.; NC – not calculated; - – sample not tested.

The acute toxicity of PAHs to green algae and daphnids has been previously correlated to the amount of LMW, hydrophilic PAHs in an aqueous mixture (Bragin et al. 2016); however, no correlation was observed in either species in this study. Similarly for metals, despite copper and zinc are primary causes of toxicity in aquatic organisms (Babich and Stotzky 1978; Mayer et al. 2011b; Howitt et al. 2014), no correlation was observed in this study (r = -0.190 and r = 0.369, respectively). Previously reported IC_{50} and IC_{10} concentrations for *R. subcapitata* used SW with various contaminant concentrations one to two orders of magnitude larger than in this study (Bragin et al. 2016). Despite these elevated concentrations, Bragin et al. (2016) also, however, noted the effects of PAHs on algae growth were limited. In this study, correlations between algae EC_{10} and contaminant concentration was only observed for cadmium, though concentrations of copper and zinc regularly exceeded CCME guidelines. As *R. subcapitata* can acclimate to aquatic concentrations between 0.5-100 µg Cu/L (Bossuyt and Janssen 2005), local algae species may accommodate higher geogenic background levels. Brix et al. (2010) identified relatively low zinc toxicity risk for brief, one-hour events and relatively significant toxicity for chronic exposures, which could explain the lack of toxicity despite a seasonal average of 237.5 µg/L. With respect to the presence of cadmium, significant cell density decrease has been observed in *R. subcapitata* (Reis et al. 2021); however, when exposed to a mixture of copper, cadmium, nickel, and zinc, significant antagonistic interactions were observed in the organism (Nys et al. 2017). This is the most likely explanation for the general lack of toxicity observed in the dissolved SW fraction.

3.2.2 Microtox Bioassay

Microtox results did not indicate a significant response in *V. fischeri* to filtered SW samples. Generally, samples diluted 50% or greater were not significantly inhibited relative to the negative control. All samples showed some luminescence inhibition relative to the negative control after 15 minutes. As expected for SW, toxicity characteristics were highly variable within samples. As a defined toxicity trend was not observed in pre-filtered SW samples, it is likely the bulk of contaminants were particle-bound and remained in sample sediment. Though potential correlations between IC_{10} and DOC, chloride, and individual metals and PAHs were examined, Pearson's correlations were only observed between the IC_{10} and aluminum (r = 0.514) or DOC (r = 0.524) concentrations.

Fulladosa et al. (2005) found metals to be toxic to *V. fischeri* in the order of mercury > silver > copper > zinc, while cobalt, cadmium, chromium(VI), arsenic(V), and arsenic(III) showed no significant toxicity.

Furthermore, in testing binary mixtures of metals, Fulladosa et al. (2005) found copper-zinc mixtures to be additively toxic while Tsiridis et al. (2006) observed a synergistic effect. Interestingly, the latter comments that all copper-zinc IC_{50} results differed significantly from theoretical predictions; when combined with mixtures of humic acids, the toxicity of the solution decreased relative to the metals-only mixture. Based on the literature and lack of a defined toxic response, it is inferred the overall mixture of metals and organic contaminants in tested SW samples produces an overall antagonistic effect relative to any single metal or PAH species: while copper and zinc concentrations in this study exceed the single-species IC_{50} concentrations for *V. fischeri* reported by Hsieh et al. (2004), other studies observed 15-min IC_{50} values at greater concentrations of varying orders of magnitude, even in the additive or synergistic mixtures (Fulladosa et al. 2005; Ghosh et al. 1996; Rossetto et al. 2014; Tsiridis et al. 2006; Utgikar et al. 2004).

3.3 Land Use Management

Land use classification data based on Figure S2 is presented in Table 3. The current study catchments comprise 33.5% of the CoS area with a total of 76.3 km^2. The two most dominant land uses in the CoS are single-family residential (SR) at 29.9% and green (GR) at 26.9% (Table 3). Industrial (IN) is the next largest usage at 14.1%, while the remaining uses all fall below 10% including multi-family residential (MR; 5.42%), roads (R; 5.38%), highways (HW; 4.17%), commercial (CM; 7.62%), and agricultural (AG; 3.74%). However, the individual distribution of land uses for each catchment differed markedly making each unique in their potential contribution to the loading of contaminants into the SSR. These individual percentages were used, along with data from Tables S2 and S3, and the loading formula provided in the Methods, to determine summer 2019 seasonal contaminant loadings for TSS, COD, Cu, Cr, Ni, Pb, Zn, and PAHs as shown in Table S9. The SCB W catchment produced the greatest seasonal loading for all parameters at 292,000 kg, 137,000 kg, 87.8 kg, 19.0 kg, 33.3 kg, 172 kg, 365 kg, and 1.07 kg, respectively. These values represent 30-33.5% of the total study loadings of 907,000 kg, 423,000 kg, 289 kg, 59.9 kg, 104 kg, 554 kg, 1,140 kg, and 3.19 kg, respectively. As the SCB W catchment comprises 32% of the study area, these loadings are roughly proportional to the land use area; the trend is similar for the Silverwood Dog Park catchment, at 23%-29% of total study catchment loading and 34% of total study area. The slightly smaller proportion of loading estimated from the Silverwood catchment is due to lesser depth of precipitation observed at local rain gauges relative to the SCB W catchment. Though the two largest catchments, Silverwood Dog Park and SCB W, differ greatly in land use (Table 3), they are similar in area; other study catchments contribute loading generally proportional to their surface area as a percent of the CoS. This agrees with previous observations that catchment area is the dominant driver of contaminant loading (Al Masum et al., 2021).

Table 3
Land use classifications of City of Saskatoon (CoS) catchments included in this study. Areas were determined from Figure S2, while acronyms for land use classifications are shown in Table S2.

Catchment Name	Area (km^2)	CoS (%)	SR (%)	MR (%)	R (%)	HW (%)	CM (%)	IN (%)	GR (%)	AG (%)
Silverwood Dog Park	25.5	11.2	0	0	4	4	0	37	55	0
Circle Dr S Bridge W	24.6	10.8	35	10	9	7	7	15	17	0
Circle Dr S Bridge E	9.58	4.20	25	5	8	8	9	25	20	0
17th St W	9.27	4.06	39	16	8	5	14	5	5	0
14th St E	3.18	1.39	54	12	9	4	10	0	8	3
23rd St W	2.73	1.20	20	6	10	6	29	25	4	0
MacPherson Ave	1.47	0.64	54	12	9	4	10	0	8	3
TOTAL	**76.3**	**33.5**	**29.9**	**5.42**	**5.38**	**4.17**	**7.62**	**14.1**	**26.9**	**3.74**

*Represented as percentage of land use over total area of the CoS, as shown by labelled catchments in Figure S1.

Inputs from roads, highways, and commercial or industrial land uses contribute significantly to high loadings. The industrial land use in the Silverwood Dog Park catchment is estimated to contribute 16-23% of loading from all 7 study catchments despite comprising 12% of the area. Similarly, the SCB E catchment, with the second-greatest industrial land use, contributes 13-17% of total study catchment loading from 12% of the area. In the 23rd St. W catchment, located in the city centre, commercial and industrial land use also dominate pollutant loadings, though road loading of COD, Cr, and Ni were comparable to loading from industrial land use. Conversely, in residential-dominant areas, roads tend to comprise the largest input of COD, TSS, Ni, and Pb. For example, roads and highways in the Light & Power catchment are each one-third the surface area of single-residential areas, yet each contribute almost 300% more COD and TSS loading (industrial land use generates twice as much per km^2). Al Masum et al. (2021) previously observed the impact of land use on CoS contaminant loading in 2017, also noting that industrial areas had the highest relative loadings.

The first flush has been correlated with significantly increased TSS concentration (Berndtsson 2014) and 25-95% contaminant removal in the first 50% of runoff volume (Lee et al. 2002). The tracing of pollutant loading across three storm events by Zhang et al. (2013) indicate a high first flush effect across COD, TN, TP, TSS, and dissolved copper and zinc. The study clearly delineated both rainfall and contaminant peaks, accomplished using intensive sampling at 5-minute intervals for the first 60 minutes of the storm. Deletic (1998) previously remarked the relatively low sampling resolutions would limit insight into the first

flush behaviour of brief, intense, 30-minute storms, which are common on the Canadian Prairies. Grab sampling indeed limited the ability of this study to interpret SW data with respect to an event volume or contamination peak. It is nonetheless obvious that the July 25 event, sampled hours after the storm as opposed to its onset, contains significantly less COD and TSS relative to other events.

While much of the TSS in these samples can be attributed to the tarring, the antecedent dry period likely also plays a role. Dry weather was observed from the July 25 event until the August 22 event, contributing to elevated pollutant loading for all catchment areas. Though the June 20 storm was the first major (>10 mm rainfall) event of the season, its TSS loading is comparable to the July 10/18 (19 mm depth reported by the CoS) and August 22 events; hourly rainfall gauge data indicates a first flush may have been missed 4 hours prior to sampling (Figure SI-B2). First flush is not a universally observed phenomenon and is influenced by land use and local topography: assuming a majority of the pollutant mass is transported in the first volume of SW (specific author definitions differ), first flushes are often not found distinctive across TSS, EC, pH, and temperature (Bertrand-Krajewski et al. 1998; Deletic 1998; Soller et al. 2005). Many studies note nonetheless that land use and storm characteristics induce a first flush effect for some contaminants such as dissolved metals (Soller et al. 2005). Due to these small-scale influences within the catchment; modeling street-level runoff and sewer flow behaviour may be the best method for estimating the catchment-wide frequency, magnitude, and spatiotemporal distribution of the first flush.

4.0 Conclusions

In general, stormwater characteristics were similar to those of previous studies, with a bulk of contamination carried by the first volume of runoff, influenced by a combination of rainfall depth, antecedent dry period, land use, and activity within the catchment. The most significant SW quality variation between events was due to road tarring activity occurring within the city prior to the August 22 event. Seasonal trends were not observed over the summer; climate conditions over the course of the study included extended dry periods and few summer storms. Though Saskatoon frequently observes its first frost in September, precipitation trends indicate SW sampling should extend into the “frost season” as well. A lack of distinctive toxicity in filtered samples, along with comparable dissolved metals and PAH values across all events, indicates much of the contamination is particle-bound, furthermore, the overall mixture of contaminants likely antagonizes the toxic mechanism of any given contaminant species. The catchment area was observed to be a dominant driver of loading; however, grab sampling strategies prohibited assessing the influence of rainfall depth or intensity on contaminant loading. More intensive sampling strategies are necessary to contextualize stormwater data in the context of contaminant and runoff volume peaks; furthermore, intensive sampling data will create more robust flow and transport models. However, this research nonetheless adds to the existing literature on cold-climate, semi-arid stormwater, contributes to local environmental quality data, and provides a preliminary snapshot into local stormwater characteristics.

Declarations

Acknowledgements

Markus Brinkmann is currently a faculty member of the Global Water Futures (GWF) program, which received funds from the Canada First Research Excellence Funds (CFREF). That authors would like to acknowledge the Natural Sciences and Engineering Research Council of Canada (NSERC) for funding this research through an Engage Grant (M.B.) and Discovery Grant (K.M.). That authors are also grateful for in-kind support from the City of Saskatoon, specifically through the active involvement of the following individuals: Mitchell McMann, Angela Schmidt, Hossein Azinfar, Sudhir Pandey, and Grant Gardner.

Ethics approval and consent to participate

Not applicable

Consent for publication

Not applicable

Availability of data and material

Not applicable

Competing interests

The authors declare that they have no competing interests

Funding

Noted under acknowledgements

Authors' contributions

HP completed all fieldwork and sample analyses. MB and KM oversaw fieldwork and sample analysis. HP produced the first draft of the manuscript; all authors contributed to the manuscript writing and editing and have read and approved the final manuscript.

References

1. “2540 SOLIDS” (2018) In *Standard Methods For the Examination of Water and Wastewater*. Standard Methods for the Examination of Water and Wastewater. American Public Health Association. https://doi.org/doi:10.2105/SMWW.2882.030
2. Food Safety M (2017) “E. Coli/Coliform Count Plates.” *3MTM PetrifilmTM*. https://www.3m.com/3M/en_US/company-us/all-3m-products/~/ECOLICT-3M-Petrifilm-E-coli-Coliform-Count-Plates/?N=5002385+3293785155&rt=rud

3. Al Masum A, Bettman N, Read S, Hecker M, Brinkmann M, McPhedran K (2021) "Urban stormwater runoff pollutant loadings: GIS land-use classification vs. sample-based predictions." *Environmental Science and Pollution Research* Under review, September 2, 2021
4. Aryal R, Vigneswaran S, Kandasamy J, Naidu R (2010) Urban Stormwater Quality and Treatment. Korean J Chem Eng 27(5):1343–1359. https://doi.org/10.1007/s11814-010-0387-0
5. Babich H, Stotzky G (1978) Toxicity of Zinc to Fungi, Bacteria, and Coliphages: Influence of Chloride Ions. Appl Environ Microbiol 36(6):906–914
6. Bäckström M, Karlsson S, Bäckman L, Folkeson L, Lind B (2004) Mobilisation of Heavy Metals by Deicing Salts in a Roadside Environment. Water Res 38(3):720–732. https://doi.org/10.1016/j.watres.2003.11.006
7. Barbosa AE, Fernandes J, and L. David (2012) Key Issues for Sustainable Urban Stormwater Management. Water Res 46(20):6787–6798. https://doi.org/10.1016/j.watres.2012.05.029
8. Berndtsson J (2014) Storm Water Quality of First Flush Urban Runoff in Relation to Different Traffic Characteristics. Urban Water Journal 11(4):284–296
9. Bertrand-Krajewski J, Chebbo G, Saget A (1998) Distribution of Pollutant Mass vs Volume in Stormwater Discharges and the First Flush Phenomenon. Water Res 32(8):2341–2356. https://doi.org/10.1016/S0043-1354(97)00420-X
10. Björklund K (2011) *THESIS FOR THE DEGREE OF DOCTOR OF PHILOSOPHY Sources and Fluxes of Organic Contaminants in Urban Runoff*. http://publications.lib.chalmers.se/records/fulltext/134241.pdf
11. Blecken G, Rentz R, Malmgren C, Öhlander B and M. Viklander (2012) Stormwater Impact on Urban Waterways in a Cold Climate: Variations in Sediment Metal Concentrations Due to Untreated Snowmelt Discharge. J Soils Sediments 12(5):758–773. https://doi.org/10.1007/s11368-012-0484-2
12. Borris M, Österlund H, Marsalek J, Viklander M (2017) An Exploratory Study of the Effects of Stormwater Pipeline Materials on Transported Stormwater Quality. Water Sci Technol 76(2):247–255. https://doi.org/10.2166/wst.2017.195
13. Bossuyt B, Janssen C (2005) Copper Regulation and Homeostasis of Daphnia Magna and Pseudokirchneriella Subcapitata: Influence of Acclimation. Environ Pollut 136(1):135–144. https://doi.org/10.1016/j.envpol.2004.11.024
14. Bragin G, Parkerton T, Redman A, Letinksi D, Butler J, Paumen M, Sutherland C, Knarr T, Comber M, and K. den Haan. 2016. “Chronic Toxicity of Selected Polycyclic Aromatic Hydrocarbons to Algae and Crustaceans Using Passive Dosing.” *Environmental Toxicology and Chemistry* 35 (12): 2948–57. https://doi.org/10.1002/etc.3479
15. Brix K, Keithly J, Santore R, DeForest D, Tobiason S (2010) Ecological Risk Assessment of Zinc from Stormwater Runoff to an Aquatic Ecosystem. Sci Total Environ 408(8):1824–1832. https://doi.org/10.1016/j.scitotenv.2009.12.004
16. Canaidan Council of Ministers of the Environment (2009) "CCME summary table: Chemical table" from http://www.ccme.ca/en/current_priorities/water/index.html

17. Charbeneau R, Barrett M (1998) Evaluation of methods for estimating stormwater pollutant loads. Water Environ Res 70(7):1295–1302
18. Chung J, Yu D, S., and Hong Y (2014) Environmental Source of Arsenic Exposure. Journal of Preventive Medicine Public Health 47(5):253–257. https://doi.org/10.3961/jpmph.14.036
19. Codling G, Yuan H, Jones PD, Giesy JP, Hecker M (2020) Metals and PFAS in stormwater and surface runoff in semi-arid Canadian city subject to large variation in temperature among seasons. Environ Sci Pollut Res 27:18232–18241
20. Curtis L, Garzon C, Arkoosh M, Collier T, Myers M, Buzitis J, Hahn M (2011) Reduced Cytochrome P4501A Activity and Recovery from Oxidative Stress during Subchronic Benzo[a]Pyrene and Benzo[e]Pyrene Treatment of Rainbow Trout. Toxicol Appl Pharmacol 254(1):1–7. https://doi.org/10.1016/j.taap.2011.04.015
21. Davis A, Shokouhian M, Ni S (2001) Loading Estimates of Lead, Copper, Cadmium, and Zinc in Urban Runoff from Specific Sources. Chemosphere 44(5):997–1009. https://doi.org/10.1016/S0045-6535(00)00561-0
22. Deletic A (1998) The First Flush Load of Urban Surface Runoff. Water Res 32(8):2462–2470. https://doi.org/10.1016/S0043-1354(97)00470-3
23. Environment Canada (1993) *Biological Test Method. Toxicity Test Using Luminescent Bacteria*. *Report EPS 1/RM/24*
24. EPA (Institution/Organization) (2002) “Method 1003.0: Green Alga, Selenastrum Capricornutum. Growth Test; Chronic Toxicity, ” no. October
25. Fulladosa E, Murat J, Martínez M, Villaescusa I (2005) Patterns of Metals and Arsenic Poisoning in Vibrio Fischeri Bacteria. Chemosphere 60(1):43–48. https://doi.org/10.1016/j.chemosphere.2004.12.026
26. Fulladosa E, Murat J, Villaescusa I (2005) Study on the Toxicity of Binary Equitoxic Mixtures of Metals Using the Luminescent Bacteria *Vibrio Fischeri* as a Biological Target. Chemosphere 58(5):551–557. https://doi.org/10.1016/j.chemosphere.2004.08.007
27. Galfi H, Österlund H, Marsalek J, Viklander M (2017) “Mineral and Anthropogenic Indicator Inorganics in Urban Stormwater and Snowmelt Runoff: Sources and Mobility Patterns.” Water Air Soil Pollution 228 (7). https://doi.org/10.1007/s11270-017-3438-x
28. Gasperi J, Zgheib S, Cladière M, Rocher V, Moilleron R, Chebbo G (2012) Priority Pollutants in Urban Stormwater: Part 2 - Case of Combined Sewers. Water Res 46(20):6693–6703. https://doi.org/10.1016/j.watres.2011.09.041
29. Ghosh, S., Doctor, P., and P. Kulkarni. 1996. “Toxicity of Zinc in Three Microbial Test Systems.” *Environmental Toxicology and Water Quality* 11 (1): 13–19. https://doi.org/10.1002/(SICI)1098-2256(1996)11:1<13::AID-TOX3>3.0.CO;2-C.
30. Göbel P, Dierkes C, and W. Coldewey (2007) Storm Water Runoff Concentration Matrix for Urban Areas. J Contam Hydrol 91(1–2):26–42. https://doi.org/10.1016/j.jconhyd.2006.08.008

31. Gunawardena J, Egodawatta P, Ayoko G, Goonetilleke A (2013) Atmospheric Deposition as a Source of Heavy Metals in Urban Stormwater. Atmos Environ 68:235–242. https://doi.org/10.1016/j.atmosenv.2012.11.062
32. HACH (2014) "Chemical Oxygen Demand, Dichromate Method." *Hach* DOC31653: 10. https://doi.org/10.1002/9780470114735.hawley03365
33. ———. 2019. "Coliforms, Total, Fecal, Coli E: Method 8074 - Membrane Filtration." *Membrane Filtration Method*, 1–14
34. Harmel D, Wagner K, Martin E, Smith D, Wanjugi P, Gentry T, Gregory L, Hendon T (2016) Effects of Field Storage Method on E. Coli Concentrations Measured in Storm Water Runoff. Environ Monit Assess 188(3):1–11. https://doi.org/10.1007/s10661-016-5183-9
35. Herngren L, Goonetilleke A, Ayoko G, Mostert M (2010) Distribution of Polycyclic Aromatic Hydrocarbons in Urban Stormwater in Queensland, Australia. Environ Pollut 158(9):2848–2856. https://doi.org/10.1016/j.envpol.2010.06.015
36. Howitt J, Mondon J, Mitchell B, Kidd T, Eshelman B (2014) Urban Stormwater Inputs to an Adapted Coastal Wetland: Role in Water Treatment and Impacts on Wetland Biota. Sci Total Environ 485–486(1):534–544. https://doi.org/10.1016/j.scitotenv.2014.03.101
37. Hsieh C, Tsai M, Ryan D, Pancorbo O (2004) Toxicity of the 13 Priority Pollutant Metals to Vibrio Fisheri in the Microtox® Chronic Toxicity Test. Sci Total Environ 320(1):37–50. https://doi.org/10.1016/S0048-9697(03)00451-0
38. Huang J, Du P, Ao C, Ho M, Lei M, Zhao D, Wang Z (2007) Multivariate Analysis for Stormwater Quality Characteristics Identification from Different Urban Surface Types in Macau. Bull Environ Contam Toxicol 79(6):650–654. https://doi.org/10.1007/s00128-007-9297-1
39. Jartun M, Ottesen R, Steinnes E, Volden T (2008) Runoff of Particle Bound Pollutants from Urban Impervious Surfaces Studied by Analysis of Sediments from Stormwater Traps. Sci Total Environ 396(2–3):147–163. https://doi.org/10.1016/j.scitotenv.2008.02.002
40. Järveläinen J, Sillanpää N, Koivusalo H (2017) Land-Use Based Stormwater Pollutant Load Estimation and Monitoring System Design. Urban Water Journal 14(3):223–236. https://doi.org/10.1080/1573062X.2015.1086005
41. Kuang X, Sansalone J (2011) Cementitious Porous Pavement in Stormwater Quality Control: PH and Alkalinity Elevation. Water Sci Technol 63(12):2992–2998. https://doi.org/10.2166/wst.2011.505
42. Lee J, Bang K, Ketchum H, Choe J, and M. Yu (2002) First Flush Analysis of Urban Storm Runoff. Sci Total Environ 293(1–3):163–175. https://doi.org/10.1016/S0048-9697(02)00006-2
43. Lee J, Bang W (2000) Characerisation of Urban Storm Water Runoff. Water Resour 34(6):1773–1780
44. Legret M, Pagotto C (1999) Evaluation of Pollutant Loadings in the Runoff Waters from a Major Rural Highway. Sci Total Environ 235(1–3):143–150. https://doi.org/10.1016/S0048-9697(99)00207-7
45. Liu A, Egodawatta P, Guan Y, Goonetilleke A (2013) Influence of Rainfall and Catchment Characteristics on Urban Stormwater Quality. Sci Total Environ 444:255–262.

https://doi.org/10.1016/j.scitotenv.2012.11.053

46. Ma Y, Egodawatta P, McGree J, Liu A, Goonetilleke A (2016) Human Health Risk Assessment of Heavy Metals in Urban Stormwater. Sci Total Environ 557–558:764–772. https://doi.org/10.1016/j.scitotenv.2016.03.067
47. Mangani G, Berloni A, Bellucci F, Tatàno F, Maione M (2005) Evaluation of the Pollutant Content in Road Runoff First Flush Waters. Water Air Soil Pollution 160(1–4):213–228. https://doi.org/10.1007/s11270-005-2887-9
48. Masoner J, Kolpin D, Cozzarelli I, Barber L, Burden D, Foreman W, Forshay K (2019) Urban Stormwater: An Overlooked Pathway of Extensive Mixed Contaminants to Surface and Groundwaters in the United States. Environ Sci Technol 53(17):10070–10081. https://doi.org/10.1021/acs.est.9b02867
49. Matos C, Bento R, Bentes I (2015) "Urban Land-Cover, Urbanization Type and Implications for Storm Water Quality: Vila Real as a Case Study." Journal of Hydrogeology Hydrologic Engineering 04 (02). https://doi.org/10.4172/2325-9647.1000122
50. Mayer T, Rochfort Q, Marsalek J, Parrott J, Servos M, Baker M, Mcinnis R, Jurkovic A, and I. Scott (2011a) Environmental Characterization of Surface Runoff from Three Highway Sites in Southern Ontario, Canada: 1. Chemistry. Water Qual Res J Can 46(2):110–120. https://doi.org/10.2166/wqrjc.2011.035
51. ———. 2011b. "Environmental Characterization of Surface Runoff from Three Highway Sites in Southern Ontario, Canada: 2. Toxicology." *Water Quality Research Journal of Canada* 46 (2): 121–36. https://doi.org/10.2166/wqrjc.2011.036
52. McCarthy D, Deletic A, Mitchell V, Diaper C (2011) Development and Testing of a Model for Micro-Organism Prediction in Urban Stormwater (MOPUS). J Hydrol 409(1–2):236–247. https://doi.org/10.1016/j.jhydrol.2011.08.023
53. McGrath J, Parkerton T, Hellweger F, Di Toro D (2005) Validation of the Narcosis Target Lipid Model for Petroleum Products: Gasoline as a Case Study. Environ Toxicol Chem 24(9):2382–2394. https://doi.org/10.1897/04-387R.1
54. McLeod S, Kells J, Putz G (2006) Urban Runoff Quality Characterization and Load Estimation in Saskatoon, Canada. J Environ Eng 132(11):1470–1481. https://doi.org/10.1061/(ASCE)0733-9372(2006)132:11(1470)
55. Melanen M (1981) "Quality of runoff water in urban areas." *Finland: National Board of Waters.*
56. Milukaite A, Šakalys J, Kvietkus K, Vosyliene M, Kazlauskiene N, Karlavičiene V (2010) Physico-Chemical and Ecotoxicological Characterizations of Urban Storm Water Runoff. Polish Journal of Environmental Studies 19(6):1279–1285
57. Mitchell G (2005) Explaining variations in public acceptability of road pricing schemes. J Environ Manage 74:1–9
58. Moghadas S, Paus K, Muthanna T, Herrmann I, Marsalek J, Viklander M (2015) Accumulation of Traffic-Related Trace Metals in Urban Winter-Long Roadside Snowbanks. Water Air Soil Pollution

226(12):1–15. https://doi.org/10.1007/s11270-015-2660-7

59. Nordeidet B, Nordeide T, Åstebøl SO, Hvitved-Jacobsen T (2004) Prioritising and planning of urban stormwater treatment in the Alna watercourse in Oslo. Sci Total Environ 334–335:231–238
60. Nys C, Regenmortel T, Janssen C, Blust R, Smolders E, De Schamphelaere K (2017) Comparison of Chronic Mixture Toxicity of Nickel-Zinc-Copper and Nickel-Zinc-Copper-Cadmium Mixtures between Ceriodaphnia Dubia and Pseudokirchneriella Subcapitata. Environ Toxicol Chem 36(4):1056–1066. https://doi.org/10.1002/etc.3628
61. Owca T, Kay M, Faber J, Remmer C, Zabel N, Wiklund J, Wolfe B, Hall R (2020) “Use of Pre-Industrial Baselines to Monitor Anthropogenic Enrichment of Metals Concentrations in Recently Deposited Sediment of Floodplain Lakes in the Peace-Athabasca Delta (Alberta, Canada).” Environ Monit Assess 192 (2). https://doi.org/10.1007/s10661-020-8067-y
62. Qinqin L, Qiao C, Jiancai D, Weiping H (2015) The Use of Simulated Rainfall to Study the Discharge Process and the Influence Factors of Urban Surface Runoff Pollution Loads. Water Sci Technol 72(3):484–490. https://doi.org/10.2166/wst.2015.239
63. Reinosdotter K, Viklander M (2005) A Comparison of Snow Quality in Two Swedish Municipalities-Luleå and Sundsvall. Water Air Soil Pollution 167(1–4):3–16. https://doi.org/10.1007/s11270-005-8635-3
64. Reis L, de Oliveira Gonçalves Alho L, de Abreu C, and M. da Graça Gama Melão. 2021. “Using Multiple Endpoints to Assess the Toxicity of Cadmium and Cobalt for Chlorophycean Raphidocelis Subcapitata.” Ecotoxicol Environ Saf 208. https://doi.org/10.1016/j.ecoenv.2020.111628
65. Rentz R, Widerlund A, Viklander M, Öhlander B (2011) Impact of Urban Stormwater on Sediment Quality in an Enclosed Bay of the Lule River, Northern Sweden. Water Air Soil Pollution 218(1–4):651–666. https://doi.org/10.1007/s11270-010-0675-7
66. Rossetto A, Pedroso Melegari S, Ouriques L, Matias W (2014) Comparative Evaluation of Acute and Chronic Toxicities of CuO Nanoparticles and Bulk Using Daphnia Magna and Vibrio Fischeri. Sci Total Environ 490:807–814. https://doi.org/10.1016/j.scitotenv.2014.05.056
67. Rossi L, Chèvre N, Fankhauser R, Margot J, Curdy R, Babut M, Barry D (2013) Sediment Contamination Assessment in Urban Areas Based on Total Suspended Solids. Water Res 47(1):339–350. https://doi.org/10.1016/j.watres.2012.10.011
68. Sakson G, Brzezinska A, Zawilski M (2018) “Emission of Heavy Metals from an Urban Catchment into Receiving Water and Possibility of Its Limitation on the Example of Lodz City.” Environ Monit Assess 190 (5). https://doi.org/10.1007/s10661-018-6648-9
69. Selvakumar A, Borst M (2006) Variation of Microorganism Concentration in Urban Stormwater Runoff with Land Use and Seasons. J Water Health 4(1):109–124. https://doi.org/10.2166/wh.2005.063
70. Soller J, Stephenson J, Olivieri K, Downing J, Olivieri A (2005) Evaluation of Seasonal Scale First Flush Pollutant Loading and Implications for Urban Runoff Management. J Environ Manage 76(4):309–318. https://doi.org/10.1016/j.jenvman.2004.12.007

71. Soto P, Gaete H, Hidalgo M (2011) “Evaluación de La Actividad de La Catalasa, Peroxidación Lipídica, Clorofila-a y Tasa de Crecimiento En La Alga Verde de Agua Dulce Pseudokirchneriella Subcapitata Expuesta a Cobre y Zinc.” Latin American Journal of Aquatic Research 39 (2): 280–285. https://doi.org/10.3856/vol39-issue2-fulltext-9
72. Taka M, Kokkonen T, Kuoppamäki K, Niemi T, Sillanpää N, Valtanen M, Warsta L, Setälä H (2017) Spatio-Temporal Patterns of Major Ions in Urban Stormwater under Cold Climate. Hydrol Process 31(8):1564–1577. https://doi.org/10.1002/hyp.11126
73. Tsiridis V, Petala M, Samaras P, Hadjispyrou S, Sakellaropoulos G, Kungolos A (2006) Interactive Toxic Effects of Heavy Metals and Humic Acids on *Vibrio Fischeri*. Ecotoxicol Environ Saf 63(1):158–167. https://doi.org/10.1016/j.ecoenv.2005.04.005
74. US EPA (1983) "Final Report of the Nationwide Urban Runoff program." vol. I. US EPA, Washington, D.C.
75. Utgikar V, Chaudhary N, Koeniger A, Tabak H, Haines J, Govind R (2004) Toxicity of Metals and Metal Mixtures: Analysis of Concentration and Time Dependence for Zinc and Copper. Water Res 38(17):3651–3658. https://doi.org/10.1016/j.watres.2004.05.022
76. Westerlund C, Viklander M (2008) Transport of Total Suspended Solids during Snowmelt - Influence by Road Salt, Temperature and Surface Slope. Water Air Soil Pollution 192(1–4):3–10. https://doi.org/10.1007/s11270-007-9579-6
77. Winter J, Desellas A, Fletcher R, Heintsch L, Morley A, Nakamoto L, Utsumi K (2011) Algal Blooms in Ontario, Canada: Increases in Reports since 1994. Lake Reservoir Management 27(2):107–114. https://doi.org/10.1080/07438141.2011.557765
78. Yang Y, Toor G (2017) Sources and Mechanisms of Nitrate and Orthophosphate Transport in Urban Stormwater Runoff from Residential Catchments. Water Res 112:176–184. https://doi.org/10.1016/j.watres.2017.01.039
79. Zawilski M, Sakson G, Brzezińska A (2014) Opportunities for Sustainable Management of Rainwater: Case Study of Łódź, Poland. Ecohydrology Hydrobiology 14(3):220–228. https://doi.org/10.1016/j.ecohyd.2014.07.003
80. Zgheib S, Moilleron R, Chebbo G (2012) Priority Pollutants in Urban Stormwater: Part 1 - Case of Separate Storm Sewers. Water Res 46(20):6683–6692. https://doi.org/10.1016/j.watres.2011.12.012
81. Zhang Q, Wang X, Hou P, Wan W, Ren Y, Ouyang Z, Yang L (2013) The Temporal Changes in Road Stormwater Runoff Quality and the Implications to First Flush Control in Chongqing, China. Environ Monit Assess 185(12):9763–9775. https://doi.org/10.1007/s10661-013-3289-x
82. Zhang Z, Hibberd A, Zhou J (2008) Analysis of Emerging Contaminants in Sewage Effluent and River Water: Comparison between Spot and Passive Sampling. Anal Chim Acta 607(1):37–44. https://doi.org/10.1016/j.aca.2007.11.024
83. Zubala T, Patro M, Boguta P (2017) Variability of Zinc, Copper and Lead Contents in Sludge of the Municipal Stormwater Treatment Plant. Environ Sci Pollut Res 24(20):17145–17152.

https://doi.org/10.1007/s11356-017-9338-1

Figures

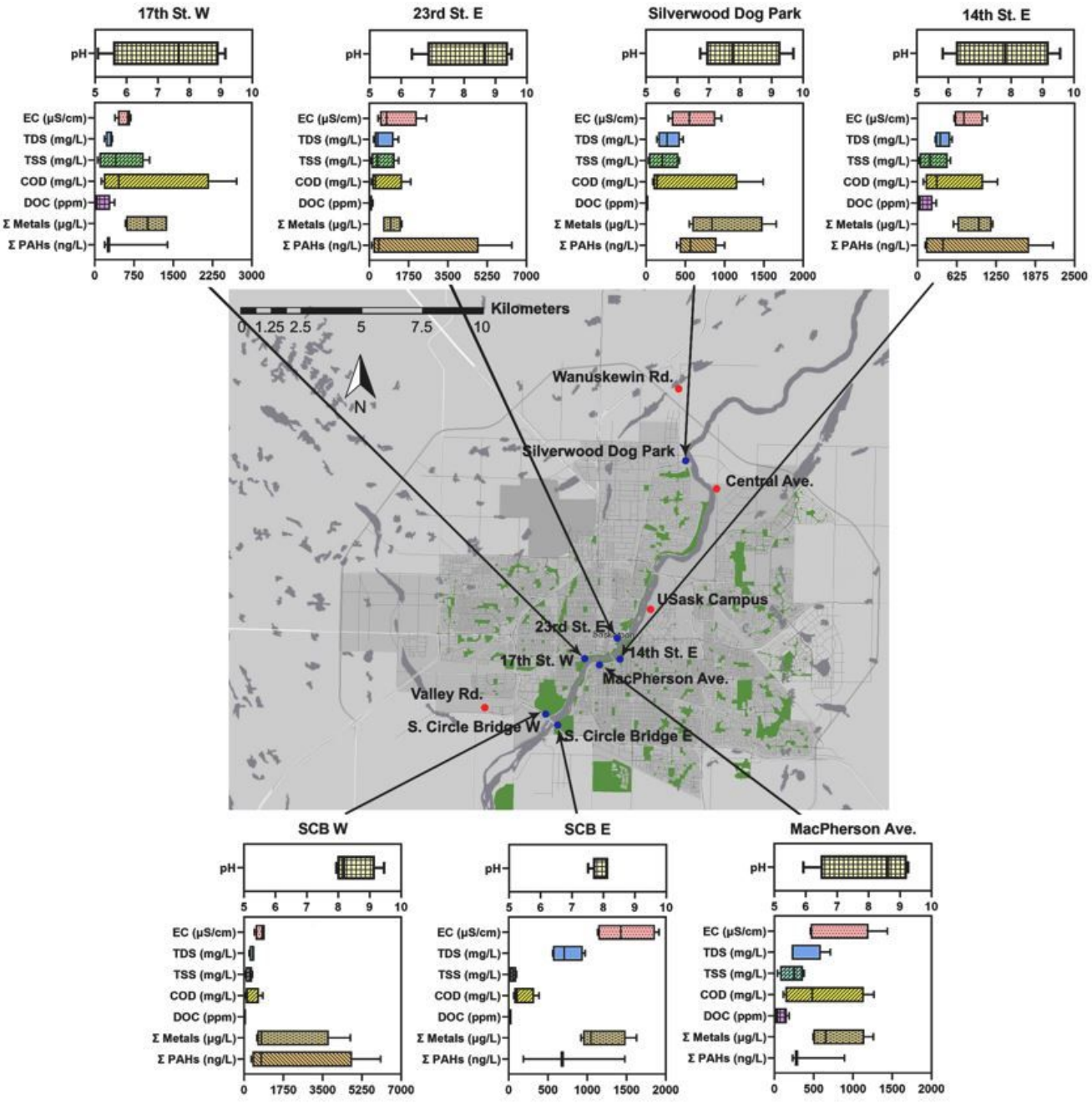

Figure 1

Map of the City of Saskatoon (CoS) and a summary of outfall stormwater (SW) data for the 2019 sampling season. SW outfalls are indicated with blue dots along the river, with red dots indicating snow

storage facilities (presented in a parallel study). Box and whisker plots indicate averages for four storm events as summarized in Table 1.

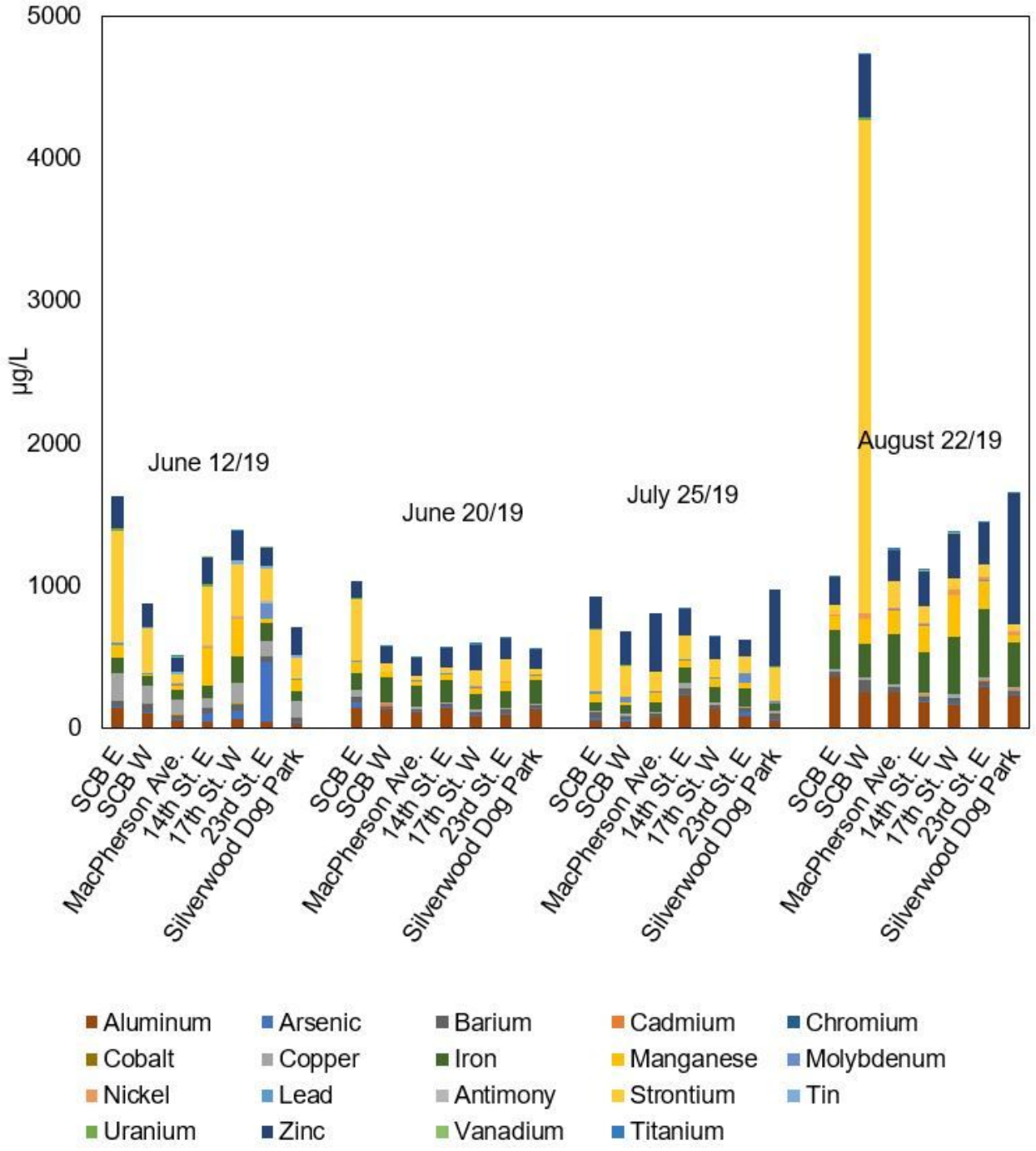

Figure 2

Average stormwater dissolved metals concentrations for four sampling dates and seven catchment areas in 2019. All sampling data values can be found in Table S7.

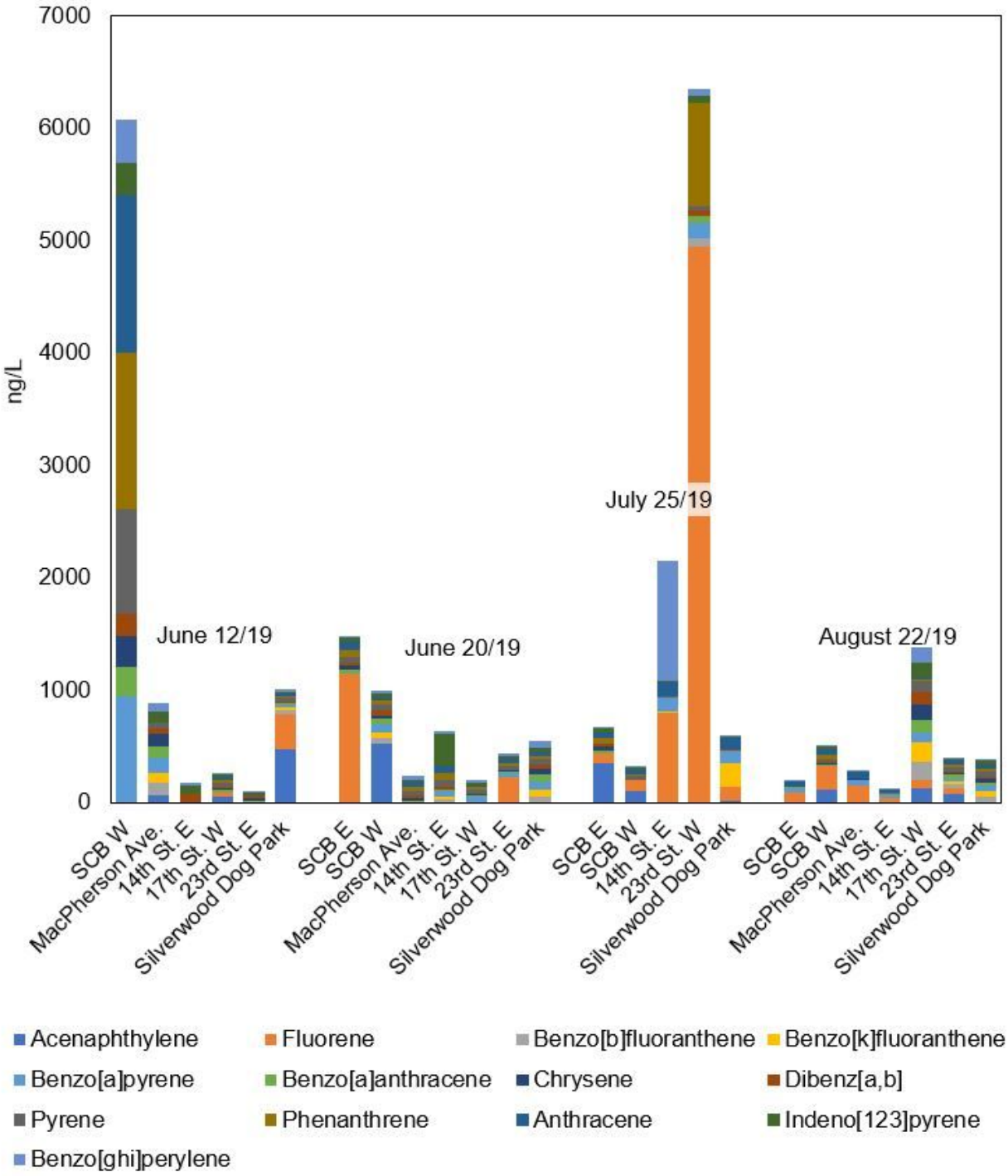

Figure 3

Average stormwater PAH concentrations for four sampling dates and seven catchment areas in 2019. All sampling data values can be found in Table S8.

Supplementary Files

This is a list of supplementary files associated with this preprint. Click to download.

- PopicketalStormwaterSIESEU.docx